URSI GASS 2021, Rome, Italy, 28 August - 4 September 2021

The Precision Radio Instrument for Antenna Measurements (PRIAM): measurement strategy

Krishna P. Makhija*(1)(2), Varundev Sukhil(1), Bang D. Nhan(2), Joanne Bechta Dugan(1), and Richard F. Bradley(1)(2)
(1) Charles L. Brown Department of Electrical and Computer Engineering, University of Virginia, Charlottesville, VA, USA
(2) National Radio Astronomy Observatory, Charlottesville, VA, USA

Abstract

The emergence of experimental 21-cm cosmology engenders unique challenges towards its instrumentation. The presence of bright *foregrounds* consisting of Galactic and extragalactic synchrotron emission several orders of magnitude higher than the expected highly-redshifted 21-cm line places high precision requirements on the antenna beam. We present an antenna calibration technique that utilizes a drone with high precision positioning and unique modulation techniques to measure the complex voltage beam of an antenna-under-test (AUT) to the required degree of precision.

1 Introduction

There has been a revival of interest in low-frequency radio astronomy instrumentation, particularly with regards to the study of emission of neutral hydrogen present in the primordial inter-galactic medium as a probe of large-scale structure evolution. The highly redshifted 21-cm line at $5 \lesssim z \lesssim 15$ can yield valuable information about the Epoch of Reionization (EOR), a phase in cosmic history during which UV radiation from the primordial stars and galaxies caused the neutral H I atoms present in the IGM to "reionize" into H II. Numerous approaches to study this highly redshifted 21-cm line are underway, all of which have primary elements operating in the VHF range [1, 2, 3]. However, the presence of bright foregrounds that are approximately a million times brighter than the cosmological signal ($T_{21\mathrm{cm}} \sim 10$ mK) engenders unique challenges for its removal, and places exquisite sensitivity requirements on the instruments.

Recently, the EDGES experiment reported for the first time an absorption feature at 78 MHz [4] in the sky-averaged high-redshift 21-cm line which has been challenged by [5] on grounds of inaccurate beam modeling and errors due to ground effects. This places a growing need for a precise calibration and measurement system for the primary element beam response.

However, due to their intrinsically large physical dimensions conventional beam-pattern measuring techniques like anechoic chambers are not viable. They also do not allow for testing *in situ* effects like soil and nearby reflective structures. Astronomical flux calibrators like Cas A are known to a limited accuracy at these frequencies and do not provide the required levels of precision for a beam map [6]. The use of low-earth orbiting sources like the Orbcomm fleet has yielded useful constraints on beam patterns but are limited to ∼138 MHz [7]. [8] used an aerial drone for calibrating the beam response of a higher frequency receiving element. [9] and [10] also used aerial drones for calibrating hydrogen observatories. However, the Orbcomm technique lacked frequency coverage whereas [8, 9] and [10] lacked phase measurements and multipath scattering corrections. [11] and [12] report techniques to map the phase of an antenna but rely on either electromagnetic simulations of the transmitting antenna or tethering the drone transmitter to the ground with an optical link for phase lock. The following paper summarizes a new approach to high precision magnitude and phase mapping via measurement alone using a drone mounted with a calibrator signal. As a test case and science motivator we will be using the feed from the Hydrogen Epoch of Reionization Array (HERA).

2 Science Objectives

The magnitude of the antenna beam response weights the spatially-varying low-frequency sky differently in different regions. The chromaticity of the beam further imposes a spectral structure on the measurement. Error propagation studies by the HERA team [13] suggest that a precision of 1% of the beam map is sufficient for detection whereas to confirm the EDGES experiment [4] at 78 MHz the precision requirement goes up to ≈ 1:4000. HERA employs a zero-delay zenith-pointing interferometer and a *delay delay-rate* filtering technique [1] for foreground removal. This causes the sources at the horizon to appear brighter leading to the well-documented "pitchfork" shape [14]. There is thus a need for making frequency-spanning precise measurements of the magnitude of the beam including sidelobes. In addition, Faraday rotation from the ionosphere causes Stokes leakage which when combined with intrinsic cross-polarization effects from the antenna can cause further confusion. The intrinsic cross-polarization ratio (IXR) of a polarimeter is given by [15]:

$$\mathrm{IXR} = \left(\frac{\kappa(\mathbf{J}_a) + 1}{\kappa(\mathbf{J}_a) - 1} \right)^2, \tag{1}$$

Where $\mathbf{J}_a$ is the 2×2 Jones matrix of the antenna, which is a composite of complex voltage gain and parallactic angle

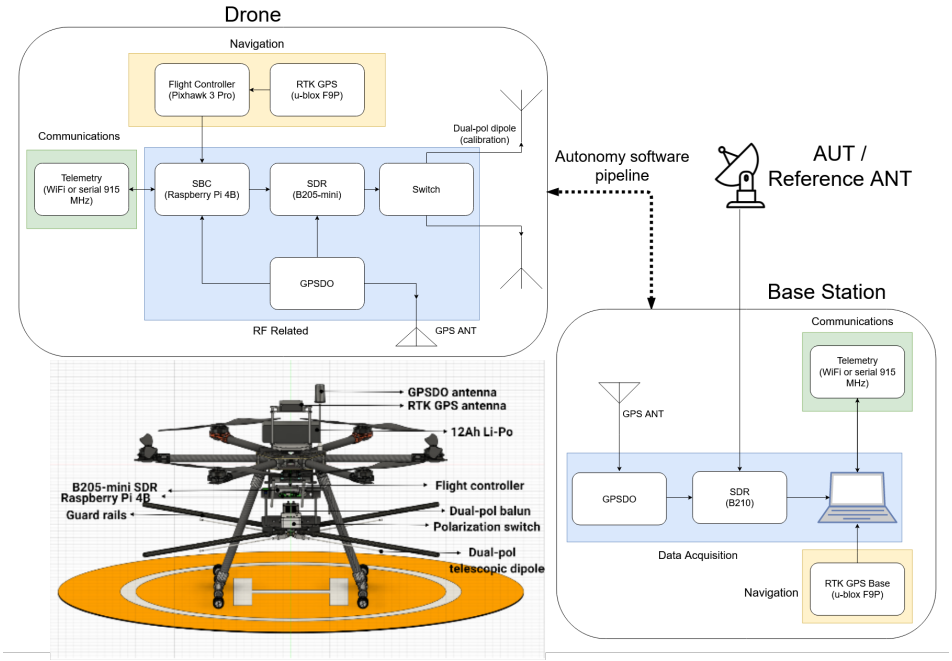

Figure 1. A top-level block diagram of the complete calibration system. Inset shows a 3D CAD render of the drone.

measurement. From the above, it becomes apparent that a precise measurement of the phase of the antenna beam is also necessary for constraining systematic effects and making a detection.

3 System Description

From the top-most level the system can be split up into two main components: a drone and a base station. The drone system consists of a Tarot T960 hexa-rotor frame with an all-up weight capacity of 12 kgs. A 12Ah battery provides about 20-30 minutes of flight time. The flight controller being used is a Pixhawk 3 Pro with a ZED-F9P RTK (real-time kinematics) GPS capable of 1-cm accuracy. The payload consists of an Ettus B205mini software-defined radio (SDR) controlled by a Raspberry Pi 4B single-board computer. A GPS disciplined oscillator (GPSDO) and separate antenna provide a 10 MHz frequency reference to the SDR. An additional RF module provides gain, filtering, and switching capability to switch between linear-X, -Y and circular polarizations. The antenna is a dual-polarized, telescopic wire-dipole tunable from 70 MHz to 1 GHz. The entire antenna assembly is to be stabilized via guard rails to the body of the drone to reduce wind loading.

The base station consists of a laptop, radio receiver and data acquisition (DAQ), GPSDO-based frequency reference, and communications to the drone. The receiver and DAQ is made up of 2 Ettus B210 SDRs each operating at 55 MSPS in single-channel mode. Another GPSDO on the ground station provides a 10 MHz reference frequency to the receiver and is used to achieve frequency coherence with the drone SDR. All of the above SDRs are tunable from 70 MHz to 6 GHz. Communications to the drone can be established via WiFi and/or 915 MHz telemetry. The test system also consists of a reference antenna similar to the one used in [7]. A complete block diagram of the system is shown in Figure 1. Nearly all the sub-systems are operated using free and open-source software: the SDRs are controlled via GNU Radio, the flight controller uses Ardupilot which is interfaced to the Raspberry Pi via a ROS (Robot Operating System) package called MAVROS. This provides one complete flexibility and control of the system. Finally, a custom-written software pipeline synchronizes the drone, receiver and transmitter and makes the entire experiment autonomous.

4 Technique

Since the beam properties of the transmitting antenna are unknown *a priori*, all beam measurements are referenced to the *reference* antenna, whose phase and magnitude are well-known and modeled *a priori*. The drone will perform several hemispherical sorties with waypoint-based (WP) navigation (Figure 2) first around the reference antenna and then around the AUT. The drone will pause at each WP and establish a handshake with the base station. The base station begins acquiring data and stops when it receives a stop trigger from the drone. The drone then moves to the next WP and the sequence is repeated. At each WP, the drone transmits 100 pulses of phase modulated signal bursts. There is thus a *discrete* sampling of the beam. Finally, the calibration signal is de-embedded from the reference antenna measurement and used to characterize the AUT in post-processing. In Jones formalism, this can be expressed as:

$$V_{\text{ref}}(r,\theta,\phi) = \mathbf{J}_t(r,\theta,\phi)\mathrm{e}_i(r,\theta,\phi)\mathbf{J}_{\text{ref}}(r,\theta,\phi), \qquad (2)$$

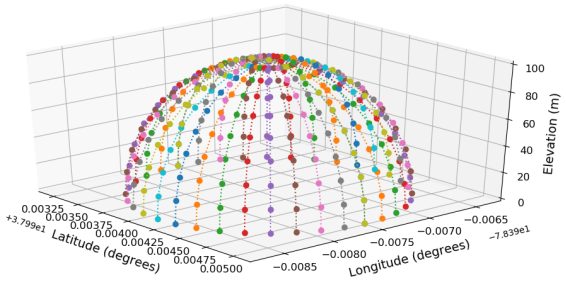

Figure 2. The proposed flight path will be a series of over-the-horizon hemispherical sorties spaced 10 degrees in azimuth. The drone will pause at every 10 degree step in elevation to execute its calibration routine. The pose of the drone will be adjusted to ensure that polarizations of the transmitting antennas are aligned with the AUT polarizations at all times so as to minimize error.

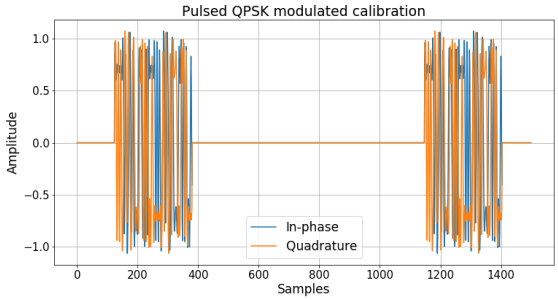

Figure 3. GNU Radio simulation of the QPSK modulated calibration signal. In this figure, the pulse ON and OFF times have been scaled down for illustration. In practice, $T_{ON+OFF} > \tau_D$, where τ_D is the largest multipath delay in the test environment.

Where V_{ref} is the voltage vector measured at the terminals of the reference antenna, $\mathbf{J}_t$, $\mathbf{J}_{\text{ref}}$ are the Jones matrices of the transmit and reference antennas, and e_i is the propagated electric field at the receiving antenna. Note that all the terms above are functions of the position of the drone, denoted by (r, θ, ϕ). The calibration signal is de-embedded from the measurement by:

$$V_{\text{ref}}\mathbf{J}_{\text{ref}}^{-1} = \mathbf{J}_t \mathrm{e}_i, \tag{3}$$

Wherein the position terms are dropped for brevity. Keeping all other conditions intact, the measurement will be repeated at the same location, this time with the AUT. The Jones matrix of the AUT will be given by:

$$\mathbf{J}_{\text{AUT}} = V_{\text{AUT}}\mathbf{J}_t \mathrm{e}_i \tag{4}$$

4.1 Phase Measurements

The equations above suggest that one can obtain both phase and magnitude measurements simultaneously. However, for making phase measurements, one still requires a reference phase and some form of signal modulation. A reference phase will be achieved using the reference antenna. Signal modulation is achieved by virtue of the discrete sampling method mentioned above, and phase modulation as described in section 4.2. However, for the phase calibration to work as intended, the *exact same* signal in phase must be transmitted to each antenna. While the SDR can, in principle, reproduce any signal defined in software, this proves to be a fairly challenging task in practice. Firstly, the frequency accuracy of the B-2xx SDR is 2 ppm which at the HERA mid-band frequency yields a frequency error of 300 Hz. Since both the receiver and transmitter have the same frequency accuracy, this yields a relative frequency offset of up to 600 Hz. In other words, there is a time-varying phase offset in each measurement. This is corrected for using GPSDOs which provide a 10 MHz reference frequency to each SDR. Since temperature control on the drone is impractical at this stage, one needs to rely on DOCXO-based GPSDOs to minimize temperature sensitivity. Secondly, since the SDR on the drone begins transmitting at an arbitrary point in time (upon arrival at WP), the phase of the LOs on the drone and base station also need to be synchronized. This is achieved by zero-padding the pre-stored waveform with a fixed length. Since both the receiver and transmitter have the same reference frequency, this ensures that the LOs will align in phase at each measurement. Since the boresight will be oversampled anyway, those data can be used to calibrate the phase of the signal during each sortie. This entire technique has been tested and validated using benchtop frequency references, SDR, and detailed software-in-the-loop (SITL) simulations of the drone flight. However, a complete integration with the drone and GPSDOs is still pending.

4.2 Precision magnitude measurements

The SDR and following RF circuitry provide a maximum TX power of 20 dBm which is required to make low-elevation sidelobe measurements of the AUT. To achieve the requirement of higher precision several error mitigation steps are in place. By transmitting a known and repeatable waveform, errors due to multipath are removed by auto-correlating the received waveform with its expected waveform *à la* a matched filter. Figure 3 above represents a simulated example of such a signal. Temperature changes in the SDRs are monitored using their respective host computers. There has been detailed temperature characterization of these instruments which will be used for corrections in post-processing. The drone's navigation consists of RTK GPS which from preliminary testing shows $\sim$10 cm of positioning accuracy in real-world flights. In addition, the host computer on the drone is interfaced with the flight controller to monitor fine variations in positioning using raw GPS data. Since the precision of the raw GPS data are 1 cm, this provides a baseline error of 1:10,000 for a 100 m sortie after corrections. Finally, the UTC offset readings from the GPSDOs are also recorded to correct for the instantaneous phase offset during calibration.

5 Current Progress and Future Work

So far, all of the sub-systems of PRIAM have been developed and tested: the drone is operational and is being tested with the autonomy software. The signal processing software has been tested separately and with detailed SITL simulations of the drone. However, a complete integration of all of the above along with pilot tests of actual antennas is still pending. We are also in the process of deploying a portable version of the Orbcomm system used in [7] to perform a cross-check with PRIAM.

6 Conclusions

The paper above presents a unique technique utilizing discrete spatial-sampling and software-defined phase modulation for making reliable and precise complex beam measurements. PRIAM's current application is towards 21-cm cosmology. However, given the open-source nature of all the software, and frequency-scalable nature of all the hardware this forms a completely flexible platform to implement other measurements for low-frequency instruments and polarimeters up to 6 GHz.

7 Acknowledgements

The authors would like to thank Prof. Jacqueline Hewitt at MIT for the generous support through grant #5215 from the Gordon and Betty Moore Foundation. Support for this work was provided by the NSF through the Grote Reber Fellowship Program administered by Associated Universities, Inc./National Radio Astronomy Observatory. We also thank the Computer Engineering department at the University of Virginia for funding support towards developing the drone and the Link Lab for use of its facilities.

References

[1] DeBoer, D. R., Parsons, A. R., Aguirre, J. E., Alexander, P., Ali, Z. S., Beardsley, A. P., ... & Cheng, C. (2017). Hydrogen epoch of reionization array (HERA). *Publications of the Astronomical Society of the Pacific*, **129**(974), 045001.

[2] Nhan, B. D., Bradley, R. F., & Burns, J. O. (2017). A Polarimetric Approach for Constraining the Dynamic Foreground Spectrum for Cosmological Global 21 cm Measurements. *The Astrophysical Journal*, **836**(1), 90

[3] Tingay, S. J., Goeke, R., Bowman, J. D., Emrich, D., Ord, S. M., Mitchell, D. A., ... & Lonsdale, C. J. (2013). The Murchison widefield array: The square kilometre array precursor at low radio frequencies. *Publications of the Astronomical Society* of Australia, **30**

[4] Bowman, J. D., Rogers, A. E., Monsalve, R. A., Mozdzen, T. J., & Mahesh, N. (2018). An absorption profile centred at 78 megahertz in the sky-averaged spectrum. *Nature*, **555**(7694), 67-70.

[5] Bradley, R. F., Tauscher, K., Rapetti, D., & Burns, J. O. (2019). A Ground Plane Artifact that Induces an Absorption Profile in Averaged Spectra from Global 21 cm Measurements, with Possible Application to EDGES. *The Astrophysical Journal*, **874**(2), 153.

[6] Cox, T. (2018). Mapping HERA's Primary Beam. *HERA Memo #49*

[7] Neben, A. R., Bradley, R. F., Hewitt, J. N., DeBoer, D. R., Parsons, A. R., Aguirre, J. E., ... & Thyagarajan, N. (2016). The hydrogen epoch of reionization array dish. I. Beam pattern measurements and science implications. *The Astrophysical Journal*, **826**(2), 199.

[8] Chang, C., Monstein, C., Refregier, A., Amara, A., Glauser, A., & Casura, S. (2015). Beam calibration of radio telescopes with drones. *Publications of the Astronomical Society of the Pacific*, **127**(957), 1131.

[9] Pupillo, G., Naldi, G., Bianchi, G., Mattana, A., Monari, J., Perini, F., ... & Aicardi, I. (2015). Medicina array demonstrator: calibration and radiation pattern characterization using a UAV-mounted radio-frequency source. *Experimental Astronomy*, **39**(2), 405-421

[10] Jacobs, D. C., Burba, J., Bowman, J. D., Neben, A. R., Stinnett, B., Turner, L., ... & Rodriguez, V. S. (2017). First demonstration of ECHO: An external calibrator for hydrogen observatories. *Publications of the Astronomical Society of the Pacific*, **129**(973), 035002.

[11] Ciorba, L., Virone, G., Paonessa, F., Matteoli, S., Bolli, P., de Lera Acedo, E., ... & Magro, A. (2019, March). Near-Field Phase Reconstruction for UAV-based Antenna Measurements. In 2019 *13th European Conference on Antennas and Propagation (EuCAP)* (pp. 1-4). IEEE.

[12] Fritzel, T., Strauß, R., Steiner, H. J., Eisner, C., & Eibert, T. (2016, October). Introduction into an UAV-based near-field system for in-situ and large-scale antenna measurements. In *2016 IEEE Conference on Antenna Measurements & Applications (CAMA)* (pp. 1-3). IEEE.

[13] Ewall-Wice, A., Dillon, J. S., Liu, A., & Hewitt, J. (2017). The impact of modelling errors on interferometer calibration for 21 cm power spectra. *Monthly Notices of the Royal Astronomical Society*, **470**(2), 1849-1870.

[14] Thyagarajan, N., Parsons, A. R., DeBoer, D. R., Bowman, J. D., Ewall-Wice, A. M., Neben, A. R., & Patra, N. (2016). Effects of antenna beam chromaticity on redshifted 21 cm power spectrum and implications for hydrogen Epoch of Reionization array. *The Astrophysical Journal*, **825**(1), 9.

[15] Carozzi, T. D., & Woan, G. (2011). A fundamental figure of merit for radio polarimeters. *IEEE Transactions on Antennas and Propagation*, **59**(6), 2058-2065.